Wefer, G., Berger, W.H., and Richter, C. (Eds.)
Proceedings of the Ocean Drilling Program, Scientific Results Volume 175

7. A Late Quaternary, High-Resolution Record of Planktonic Foraminiferal Species Distribution in the Southern Benguela Region: Site 1087[1]

Jacques Giraudeau,[2] Catherine Pierre,[3] and Laurence Herve[2]

ABSTRACT

Planktonic foraminiferal assemblages from the upper Pleistocene part of Hole 1087A (0 to 12.1 meters below seafloor) are investigated to assess the role of global and local climate changes on surface circulation in the southern Benguela region. The benthic stable isotope record indicates that the studied interval is representative of the last four climatic cycles, that is, down to marine isotope Stage (MIS) 12. The species assemblages bear a clear transitional to subpolar character, with *Neogloboquadrina pachyderma* (d), *Globorotalia inflata*, and *Globigerina bulloides,* in order of decreasing abundance, as the dominant taxa. This species association presently characterizes the mixing domain of old upwelled and open ocean waters, seaward of the Benguela upwelling cells. Abundance variation of the dominant foraminiferal species roughly follows a glacial–interglacial pattern down to MIS 8, suggesting an alternation of upwelling strength and associated seaward extension of the belt of upwelled water as a response to global climate changes. This pattern is interrupted from ~250 ka down to MIS 12, where the phase relationship with global climate is ill defined and might be interpreted as a local response of the southern Benguela region to the mid-Brunhes event. Of particular interest is a single pulse of newly upwelled waters at the location of Site 1087 during early MIS 9 as indicated by a peak abundance of sinistral *N. pachyderma* (s). Variable input of warm, salty Indian Ocean thermocline waters into the southeast Atlantic, a key component of the Atlantic heat conveyor, is indicated by abundance changes

[1] Giraudeau, J., Pierre, C. and Herve, L., 2001. A late Quaternary, high-resolution record of planktonic foraminiferal species distribution in the southern Benguela region: Site 1087. *In* Wefer, G., Berger, W.H., and Richter, C. (Eds.), *Proc. ODP, Sci. Results,* 175, 1–26 [Online]. Available from World Wide Web: <http://www-odp.tamu.edu/publications/175_SR/VOLUME/CHAPTERS/SR175_07.PDF>. [Cited YYYY-MM-DD]
[2] Département Géologie et Océanographie, UMR5805 CNRS, Université Bordeaux I, Avenue des Facultés, 33405 Talence cedex, France. giraudeau@geocean.u-bordeaux.fr
[3] LODYC, UMR121 CNRS, Université Pierre et Marie Curie, 4 Place Jussieu, 75252 Paris, France.

Initial receipt: 18 February 2000
Acceptance: 14 September 2000
Web publication: 6 April 2001
Ms 175SR-225

of the tropical taxon *Globorotalia menardii*. From this tracer, we suggest that interocean exchange was hardly interrupted throughout the last 460 k.y., but was most effective at glacial terminations, particularly during Terminations I and II, as well as during the upper part of MIS 12. This maximum input of Indian Ocean waters around the southern tip of Africa is associated with the reseeding of *G. menardii* in the tropical Atlantic.

INTRODUCTION

The southern Benguela region, which extends along the western flank of southern Africa from the Orange River mouth to the Cape of Good Hope, is one of the most complex hydrological systems of the South Atlantic. There, the nature of surface and intermediate waters is under the influence of three distinct processes (e.g., Shannon, 1985): (1) upwelling of cold, nutrient-rich South Atlantic central water from the combination of the equatorward Benguela drift and the prevailing southerly winds, (2) input of warm, salty Indian thermocline waters and rings, which are shed from the Agulhas Current retroflection area, and (3) variable admixture of Southern Ocean waters induced by instabilities in the region of the Subtropical Convergence (Fig. **F1**). These last two phenomena may allow the transfer of allochthonous planktonic fauna from Indian subtropical and Atlantic subantarctic water masses to a region otherwise characterized by populations adapted to the coastal upwelling regime.

Exploring the Neogene and Quaternary history of these Indian and subantarctic surface-water advections and, ultimately, assessing the implications for the glacial–interglacial heat balance between the South and the North Atlantic were the primary objectives for drilling at Site 1087. This site, located in the southernmost area of the Cape Basin in 1371-m-deep water (31°28′, 15°19′E), is presently affected by wind-induced upwelling that carries a clear seasonal pattern, with the maximum upwelling occurring during spring and summer (Lutjeharms and Meeuwis, 1987). This seasonal pattern is determined by the combined seasonal latitudinal shifts of the South Atlantic high-pressure system and east-moving cyclones in the south. The seasonal nature of upwelling in the southern Benguela region most probably accounts for the overall lower phytoplankton biomass in surface waters (Brown et al., 1991) compared to the situation in the north, where upwelling is perennial. Sediments over the continental margin off the Olifants River, where Site 1087 was drilled, are therefore carbonate rich and organic carbon and opal poor (Rogers and Bremner, 1991), accumulating at an average rate of 2 to 7 cm/k.y., compared to 10 to 20 cm/k.y. off Namibia (Giraudeau et al., 1998). Site 1087 recovered a relatively continuous pelagic section to 430 meters below seafloor (mbsf), spanning the last 9 m.y.

The generally high abundance and good preservation of calcareous microfossils contained in sediments at Site 1087, coupled with recent studies that document the reliability of planktonic foraminifers as tracers of present surface-water masses in the southeast Atlantic (Giraudeau, 1993; Niebler and Gersonde, 1998), indicate that the downcore distribution of species assemblages may allow for precise reconstruction of surface circulation changes around the southern tip of Africa.

F1. Schematic circulation setting around southern Africa and location of Site 1087, p. 13.

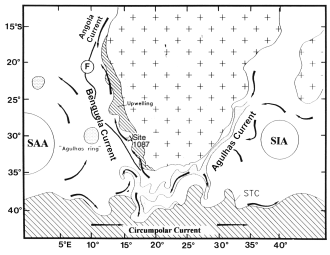

Here we report on census counts of planktonic foraminifers at Site 1087 that are representative of the last four glacial–interglacial cycles. High-resolution sampling coupled with benthic stable isotope stratigraphy provide the necessary data to reconstruct the evolution of the southern Benguela region and adjacent regions throughout the last 460 k.y.

METHODS

Taken from the top 12.1 mbsf of Hole 1087A, 193 samples (Samples 175-1087A-1H-1, 0–1 cm, through 2H-3, 90–91 cm) were examined for their planktonic foraminiferal content. Based on the preliminary age determinations from shipboard biostratigraphy and magnetostratigraphy (Shipboard Scientific Party, 1998), we chose a sampling resolution of 5 cm (Core 1H) to 10 cm (Core 2H) to reach a time resolution close to 3 k.y.

Planktonic foraminifers were obtained by disintegrating a 10-cm^3 sample and washing it over a 125-µm sieve. The samples were dried and examined under the binocular microscope, and planktonic foraminifers were identified to species level from splits of the 125-µm fraction. This size fraction was chosen for the purpose of comparison with previously published census counts at locations close to Hole 1087A (Giraudeau, 1993; Little et al., 1997; Niebler and Gersonde, 1998), as well as to promote the environmental significance of typically small polar and subpolar species (e.g., *N. pachyderma* (s) and *Globigerina quinqueloba*) that are particularly abundant on the continental shelf of the southern Benguela region (Giraudeau, 1993).

An average of 250 specimens per sample were identified following the classical taxonomic concepts of Bé (1967), Parker (1962), and Hemleben et al. (1989). In addition, the intergrades between *Neogloboquadrina dutertrei* and *N. pachyderma* (s) (P-D intergrade of Kipp, 1976) were combined with *N. pachyderma* (d). Finally, *G. menardii* ssp. and *Globorotalia tumida* were combined into the single taxonomic category *G. menardii*. With the exception of this last species group, all raw counts (Table **T1**) were transformed into relative abundances. Because of the scarcity of *G. menardii* in species assemblages at Site 1087, but considering its importance as a potential tracer of tropical/subtropical waters of Indian Ocean origin (e.g., Berger and Wefer, 1996), we conducted a separate count of this species on the total unsplit >125-µm fraction. We subsequently expressed *G. menardii* abundance as both concentration (number of specimens/gram bulk sediment) and accumulation rate (AR) (number of specimens/cm/k.y.) (Table **T2**) following the formula:

$$AR = \text{concentration} \times SR \times DBD,$$

where

SR (sedimentation rate in centimeters per thousand years) = sedimentation rate after conversion of original depth in mbsf into corrected depth in meters composite depth (Shipboard Scientific Party, 1998) and construction of the final age model, and

DBD (dry bulk density in grams per cubic centimeter) = 2.65 × (gamma-ray attenuation bulk density – 1)/(2.65 – 1).

T1. Census counts of planktonic foraminifers, p. 17.

T2. Concentrations and accumulation rates of *G. menardii*, p. 23.

Finally, we evaluated the coiling ratio of *Globorotalia truncatulinoides* (expressed as the ratio of dextral specimens vs. the sum of dextral + sinistral specimens) in conducting a separate count of this species in the total unsplit >125-µm fraction.

The stratigraphic framework is based upon the benthic foraminiferal $\delta^{18}O$ record of *Cibicidoides wuellerstorfi,* which was correlated with the SPECMAP standard record (Imbrie et al., 1984). Details of the analytical procedure are given elsewhere (Pierre et al., **Chap. 12,** this volume). Twenty stable isotope events were identified between 0 and 13 mbsf (Table **T3**; Fig. **F2**). The final age model was achieved by linear interpolation between age-control points.

T3. Age control points for the benthic foraminiferal oxygen isotope record, p. 25.

F2. Oxygen isotope depth profile, p. 14.

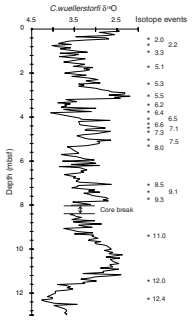

RESULTS

Distributional Trends of Dominant and Subordinate Taxa

Summary statistics of the planktonic foraminiferal census counts are given in Table **T4**. Throughout the studied part of Hole 1087A, species assemblages bear a clear transitional to subpolar character. A total of 17 taxa (excluding the *G. menardii* complex) were identified in the >125-µm fraction. Of these, eight occur with a maximum frequency >5% and an average frequency >1%. They are, in order of decreasing average abundance, *N. pachyderma* (s) (d), *G. inflata*, *G. bulloides*, *G. quinqueloba, Globigerinita glutinata, G. truncatulinoides, Globigerinoides ruber,* and *N. pachyderma* (s).

T4. List of planktonic foraminiferal taxa, p. 26.

This ranking, in terms of species dominance, is consistent with the distribution of planktonic foraminiferal species in surface sediments in the vicinity of the studied site. Site 1087 is presently located below the main Benguela drift, seaward of the boundary of active coastal upwelling, within a mixing domain of old upwelled and oligotrophic waters (Fig. **F1**). This ill-defined frontal region is characterized by a typical modern assemblage of *G. inflata* and *G. bulloides,* with common *N. pachyderma* (d), which extends equatorward up to Walvis Ridge, with a tendency for seaward deflection off Namibia related to a seaward extension of the filamentous regime north of 27°S (Giraudeau, 1993). *N. pachyderma* (d) and *G. bulloides* presently define this filamentous regime of mesotrophic, old-upwelled waters, whereas *G. inflata* is the indigenous species of the transitional faunal zone, which in the southeast Atlantic, extends in an equatorward direction along the Benguela drift (Niebler and Gersonde, 1998).

Within the interval representative of the last ~250 k.y., both dominant and subordinate taxa display a general glacial–interglacial trend in abundance changes (Fig. **F3**). Peak interglacials are associated with maximum abundances of *G. inflata*, close to Holocene values, with significant contribution of *G. bulloides*, whereas glacial intervals and cold substages within interglacial periods are characterized by an association dominated by the cold end-members of the planktonic foraminiferal assemblage, namely *N. pachyderma* (d) and, to a lesser extent, *G. quinqueloba*. This last association contains a significant contribution of *G. glutinata*. This general trend down to MIS 8 suggests a glacial–interglacial alternation of either upwelling strength and associated seaward extension of the belt of mature upwelled waters, advection of subantarctic water along the path of the Benguela drift, or a combination of both. Considering that *N. pachyderma* (s) is presently abundant in continental

F3. Relative abundances of the eight major species of planktonic foraminifers, p. 15.

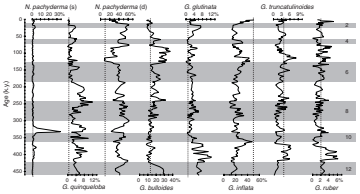

shelf sediments below the main upwelling cells (Giraudeau, 1993), the near absence of this species throughout this 250-k.y. interval suggests that any glacial pulses in upwelling strength were not sufficient to induce the presence of newly upwelled waters at the location of Site 1087.

The interval from MIS 8 to MIS 12 shows a series of complex faunal distributional trends as well as short-term events that are clearly unrelated to the general pattern observed during the past 250 k.y. (Fig. F3). Abundance changes of the dominant three taxa, *N. pachyderma* (d), *G. inflata,* and *G. bulloides,* do not follow the glacial–interglacial pattern described earlier. *G. inflata* displays a single abundance peak at the MIS 10/11 boundary, as well as a general tendency for highest concentrations in glacial intervals (with the exception of MIS 12). Similarly, peak abundances of *N. pachyderma* (d) seem to be restricted to isotope stage boundaries (i.e., MIS 9/8 boundary), as well as to the early phase of interglacial stages (i.e., early MIS 11). Finally, *G. bulloides* abundance fluctuates only slightly around Holocene values throughout MIS 8 to 11 but shows an abrupt increase during glacial MIS 12. Among the subordinate species, the subpolar and coastal upwelling species *G. quinqueloba,* which is a minor component of the faunal assemblages representative of the last 200 k.y. at Site 1087, reaches high concentrations well above the Holocene level throughout MIS 7 to 12, with significant peaks irrespective of the glacial–interglacial succession. Perhaps the most dramatic short-term event recorded within the lower half of the studied section is the single abundance peak of *N. pachyderma* (s) during early MIS 9. This maximum concentration of the cold end-member of the planktonic foraminiferal assemblage at Site 1087 is associated with high abundance of *G. quinqueloba,* which in the southern Benguela region forms with *N. pachyderma* (s) the pair of dominant taxa in surface sediments of the inner and middle shelf below coastal upwelling cells (Giraudeau and Rogers, 1994).

Contrary to the major species discussed above, *G. truncatulinoides* and *G. ruber* display a rather straightforward distributional trend with regard to the glacial–interglacial cyclicity throughout the last 460 k.y. Both species show highest concentrations at or above Holocene values during warm climatic stages. *G. truncatulinoides* is a deep-dwelling species that, in the Benguela region, is usually associated with *G. inflata* as the pair of taxa representative of oligotrophic offshore water (Giraudeau and Rogers, 1994), both species defining the transitional faunal zone in the deep South Atlantic (Bé and Tolderlund, 1971). *G. ruber* is the warm end-member of the Benguela faunal community and rarely exceeds 2% of the total foraminiferal assemblages in sediments of the southern Benguela region (Giraudeau, 1993). The common maximal occurrence of *G. ruber* and *G. truncatulinoides* during warm climatic stages should point to the presence of stratified, warmer surface waters over Site 1087. Although this interpretation may hold true for the last 250 k.y., an interval when other major species suggest a relaxation of the upwelling process during interglacials, this interpretation is too simplistic for the time period prior to MIS 7 when the overall planktonic foraminiferal assemblage shows contradictory patterns.

G. menardii and Related Proxies of Tropical-Subtropical Surface Waters

The relatively low number of taxa identified at Site 1087 is in part due to the lack of key tropical species, such as *Pulleniatina obliquiloculata, Sphaeroidinella dehiscens,* and *Globigerinoides conglobatus,* in the lo-

cal environment of the southern Benguela region. The absence of these species, which are otherwise part of the extant and fossil assemblages of the northern Benguela region (Ufkes et al., 1998; Giraudeau, 1993), as well as of the nearby South Atlantic and South Indian subtropical gyres (Bé and Tolderlund, 1971; Bé and Hutson, 1977), suggests that dramatic hydrological situations associated with extreme surface warming did not occur at the location of Site 1087 during the past 460 k.y. In other words, neither long-term eastward shifts of the subtropical water masses associated with a near-complete relaxation of the coastal upwelling process and Benguela Current drift nor massive inflows of Indian Ocean water around the southern tip of Africa are detectable from our record at the studied time resolution of 2 to 4 k.y.

We do know, however, that substantial leakage of Indian tropical water past the southern tip of Africa, due to large Agulhas rings and filaments, is part of the present circulation pattern of the South East Atlantic (e.g., Lutjeharms, 1996), and that this mechanism is believed to be a key modulator of the Atlantic heat conveyor (Gordon, 1985). The near absence of tropical species at Site 1087 is not so anomalous in that remote sensing studies clearly show that the path of Agulhas-shed rings past the Cape of Good Hope lies along a southeast-northwest track, well offshore of the continental margin (Lutjeharms and Gordon, 1987).

G. menardii, as other tropical species, is negligible in terms of contribution to the foraminiferal assemblages at Site 1087 (<0.5 wt% throughout the studied interval). A separate observation of the whole, unsplit >125-µm fraction, however, indicates that specimens of *G. menardii,* although rare in abundance, are near-continuously present at Site 1087 throughout the last 460 k.y. (Fig. **F4**). This presence has major implications. If, as suggested by others (Berger and Vincent, 1986; Charles and Morley, 1988), this species is a reliable tracer of interocean exchange south of Africa, it is likely that the "Cape Valve" was hardly closed throughout the last four climatic cycles, or alternatively, that regardless of the volume of Indian Ocean waters transferred to the Atlantic, leakages to the southern Benguela have not stopped since MIS 12.

The downcore pattern of accumulation rate of *G. menardii* at Site 1087 (Fig. **F4A**) is enlightening in view of the late Quaternary succession of this taxon in the tropical and subtropical Atlantic (Ericson and Wollin, 1968). Although the extinction of *G. menardii* in the tropical Atlantic during certain glacial intervals (i.e., during the last glacial = biozone Y, or during the upper part of MIS 6 = biozone W) is still an enigma, it has been proposed that Indian to Atlantic Ocean leakage of surface water is a plausible mechanism for reseeding this taxon during warm periods (Berger and Wefer, 1996). To our knowledge, our record is the first evidence for such a mechanism. Accumulation rates of *G. menardii* show short-term distinct peaks that are synchronous with the position of the U/V, W/X, and Y/Z zonal boundaries. If one assumes empirically that the accumulation rate of this species is a function of the volume of Indian Ocean water leakage in the southeast Atlantic, then we might surmise that *G. menardii* reseeding of the tropical Atlantic is indeed directly tied to maximum interocean exchange south of Africa.

Besides events of peak accumulation of *G. menardii* at the above mentioned zonal boundaries, an interval of high concentrations of this taxon is evident from MIS 10 to MIS 12 (Fig. **F4A**). Here, long-term intervals of maximum interocean exchange are expressed particularly during MIS 11 and 12 and are associated with distinct foraminiferal in-

F4. Concentrations and accumulation rates of *G. menardii*, p. 16.

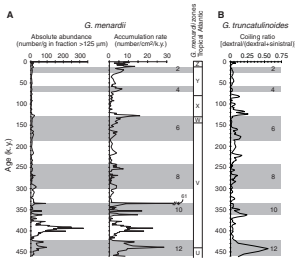

dications of extended warming periods. The ~20-k.y. interval of peak accumulation of *G. menardii* during MIS 12 is marked by the single occurrence throughout the last 460 k.y. of dominantly dextral *G. truncatulinoides* at Site 1087 (Fig. **F4B**). Dextral *G. truncatulinoides* is found preferentially in tropical water masses of the Indian and Atlantic Oceans (Bé and Tolderlund, 1971), whereas surface sediment studies indicate that the 21°C surface summer isotherm roughly defines the northernmost boundary of dominantly sinistrally coiled specimens in the South Atlantic (Niebler and Gersonde, 1998). The co-occurrence of *G. menardii* and dextral *G. truncatulinoides* during MIS 12 therefore traces the presence of tropical waters over Site 1087 throughout what is commonly considered to be one of the most extreme glacial intervals of the late Quaternary in the Southern Ocean (Hodell, 1993; Howard and Prell, 1994).

The following interval of high *G. menardii* accumulation at Site 1087 during MIS 11 (Fig. **F4A**) is associated with a high contribution to the total assemblage of the subtropical species *G. ruber* (Fig. **F3**). Contrary to the previous MIS 12 period, *G. truncatulinoides* coiling is predominantly sinistral (Fig. **F4B**). In the absence of additional information from independent proxies, we can only assume that mechanisms responsible for the MIS 12 and 11 intervals of mixed-layer warming over Site 1087 were different, these differences being in part driven by the extreme gradients in surface-water temperature and by associated latitudinal shifts of hydrological and atmospheric boundaries in the Southern Ocean across these two climatic stages (Howard and Prell, 1994; Hodell, 1993).

SUMMARY

This preliminary description of planktonic foraminiferal distribution at Site 1087 during the last four climatic cycles suggests that the surface hydrology of the southern Cape Basin off southern Africa was affected by a complex series of both short- and long-term drastic variations. The studied site lies at the crossroads of three distinct oceanographic realms, namely, the Southern Ocean, the Benguela coastal upwelling system, and the southwest Indian Ocean, which presently influence to a large extent the nature of the surface mixed layer in the southern Benguela region (Shannon and Nelson, 1996). Consequently, we argue that proxy data measured at Site 1087 can hardly provide on their own firm answers about the mechanisms that drive the hydrographic changes recorded in this study and that subsequent studies will have to rely deeply upon information gained from previous or ongoing paleoceanographic studies conducted in the above-mentioned nearby realms. Of particular relevance in this respect are investigations of Ocean Drilling Program (ODP) Site 704 (Hodell, 1993) and ODP Leg 177 (Shipboard Scientific Party, 1999) in the Atlantic part of the Southern Ocean, studies by Flores et al. (1999), Acheson et al. (1999), Rau et al. (1999) in sediment cores from the Agulhas retroflection region, and the outcomes from investigations of Leg 175 material in the Benguela coastal upwelling region (Shipboard Scientific Party, 1998, and this volume).

Among the various questions raised by this preliminary investigation, future works should particularly address the following aspects. First, the downcore distributional trend of the dominant planktonic foraminiferal species responds roughly in phase with global climate change down to MIS 8 but shows an ill-defined relationship with the glacial–interglacial cycles from ~250 k.y. to the end of the studied inter-

val of Site 1087 (i.e., MIS 12). This shift in distributional trend might be at least in part viewed as a local response of the southern Benguela productivity and circulation pattern to the so-called mid-Brunhes event (Jansen et al., 1986), a global climate oscillation of unknown origin, the manifestation of which included major changes in the whole-ocean carbon inventory and in the nature of intermediate and deep water masses (Howard and Prell, 1994).

Second, a single pulse of newly upwelled waters over Site 1087 is recorded during the early phase of MIS 9. This unique event has recently been documented with a similar micropaleontological signature (peak occurrence of *N. pachyderma* (s) in a nearby piston core (MD 962085) collected on the continental slope off the Orange River, ~2° north of Site 1087 (M.-T. Chen, pers. comm., 1999), confirming the reality of this signal in terms of surface-water changes (i.e., the observed micropaleontological signature is not related to processes of downslope transfer of shelf material). Equatorward advection of cold, *G. pachyderma* (s)-rich polar waters along southwest Africa can hardly be inferred as a mechanism for this anomalous cooling at Site 1087. Previous paleoceanographic investigations conducted in the Southern Ocean indicate that, together with MIS 11, MIS 9 was one the warmest climatic stages of the last 500 k.y. These two interglacials are characterized by extreme poleward shifts of the Polar Frontal Zone and Subtropical Convergence (Howard and Prell, 1992; Niebler, 1995), a process that acts against the presence of polar waters at the latitude of the studied site. Possible mechanisms of the recorded MIS 9 upwelling pulse at Site 1087 might include an extreme southward position of the South Atlantic high-pressure cell and associated southeasterlies and/or drastic changes in the physico-chemical nature of the upwelled waters. Detailed mapping of hydrological and atmospheric conditions during MIS 9 along the whole margin of southwest Africa presently affected by coastal upwelling will greatly improve our understanding of this short-term event.

Finally, we show that input of warm, salty Indian Ocean thermocline waters to the South East Atlantic was most effective at glacial terminations, the maximum pulses of interocean exchange being associated with reseeding of *G. menardii* in the tropical Atlantic Ocean during Terminations I and II, as well as during the upper part of MIS 12. Whether the input of Indian Ocean thermocline water is controlled mainly by the latitudinal position of the Subtropical Convergence, by changes in volume transport of the Agulhas Current along southeast Africa, which is thought to control the zonal position of the Agulhas retroflection regime (Shannon et al., 1990), or by a combination of both mechanisms is still a matter of debate. Understanding the late Quaternary timing and causes of the observed variability of Indian water inflow will therefore benefit from additional studies looking both at the dynamics of hydrological fronts in the Southern Ocean and at the circulation changes along Southeast Africa (velocity of the Agulhas Current and associated atmospheric circulation in the Southwest Indian Ocean).

ACKNOWLEDGMENTS

We thank the captain, crew, and ODP staff for their tremendous effort in recovering a record 8000 m of sediments during Leg 175. J.G. is indebted to the co-chiefs and fellow shipboard scientists for their continuous support and friendship during and after the cruise. Funding to

J.G. and C.P. by INSU/CNRS is gratefully acknowledged. The manuscript profited from the reviews of C. Richter, G.H. Scott, and P.G. Quilty. This is DGO-UMR CNRS 5805 EPOC contribution number 1354.

REFERENCES

Acheson, R., Schneider, R.R., and Kroon, D., 1999. High resolution planktonic foraminiferal records from the Southern Cape basin: evidence for regional and global climate change. European Union of Geosciences 10, March–April 1999. *J. Conf. Abstracts,* 4:211.

Bé, A.W.H., 1967. Foraminifera families: *Globigerinidae* and *Globorotalidae. In* Fraser, J.H. (Ed.), *Fisches d'Identification du Zooplankton*. Conseil Perm. Internat. Explor. Mer, Charlottenlund, Denmark, Sheet 108:1–8.

Bé, A.W.H., and Hutson, W.H., 1977. Ecology of planktonic foraminifera and biogeographic patterns of life and fossil assemblages in the Indian Ocean. *Micropaleontology,* 23:369–414.

Bé, A.W.H., and Tolderlund, D.S., 1971. Distribution and ecology of living planktonic foraminifera in surface waters of the Atlantic and Indian Oceans. *In* Funnel, B.M., and Riedel, W.R. (Eds.), *The Micropaleontology of Oceans:* Cambridge (Cambridge Univ. Press), 105–149.

Berger, W.H., and Vincent, E., 1986. Sporadic shutdown of North Atlantic deep water production during the Glacial-Holocene transition? *Nature,* 324:53–55.

Berger, W.H., and Wefer, G., 1996. Expeditions into the past: paleoceanographic studies in the South Atlantic. *In* Wefer, G., Berger, W.H., Siedler, G., Webb, D.J. (Eds.), *The South Atlantic: Present and Past Circulation:* Berlin (Springer-Verlag), 363–410.

Briskin, M., and Berggren, W.A., 1975. Pleistocene stratigraphy and quantitative paleo-oceanography of tropical North Atlantic core V216-205. *In* Saito, T., and Burckle, L.H. (Eds.), *Late Epoch Boundaries*. Micropaleontology, Spec. Publ., 1:167–198.

Brown, P.C., Painting, S.J., and Cochrane, K.L., 1991. Estimates of phytoplankton and bacterial biomass and production in the northern and southern Benguela ecosystem. *S. Afr. J. Mar. Sci.,* 11:537–564.

Charles, C.D., and Morley, J.J., 1988. The paleoceanographic significance of the radiolarian Didymocyrtis tetrathalamus in eastern Cape Basin sediments. *Palaeogeogr., Palaeoclimatol., Palaeoecol.,* 66:113–126.

Ericson, D.B., and Wollin, G., 1968. Pleistocene climates and chronology in deep-sea sediments. *Science,* 162:1227–1234.

Flores, J.-A., Gersonde, R., and Sierro, F.J., 1999. Pleistocene fluctuations in the Agulhas Current retroflection based on the calcareous plankton record. *Mar. Micropaleontol.,* 37:1–22.

Giraudeau, J., 1993. Planktonic foraminiferal assemblages in surface sediments from the southwest African continental margin. *Mar. Geol.,* 110:47–62.

Giraudeau, J., Christensen, B.A., Hermelin, O., Lange, C.B., Motoyama, I., and Shipboard Scientific Party, 1998. Biostratigraphic age models and sedimentation rates along the southwest African margin. *In* Wefer, G., Berger, W.H., and Richter, C., et al., *Proc. ODP, Sci. Results,* 175: College Station, TX (Ocean Drilling Program), 543–546.

Giraudeau, J., and Rogers, J., 1994. Phytoplankton biomass and sea-surface temperature estimates from sea-bed distribution of nannofossils and planktonic foraminifera in the Benguela Upwelling System. *Micropaleontology,* 40:275–285.

Gordon, A.L., 1985. Indian-Atlantic transfer of thermocline water at the Agulhas retroflection. *Science,* 227:1030–1033.

Hemleben, C., Spindler, M., and Anderson, O.R., 1989. *Modern Planktonic Foraminifera:* Berlin (Springer-Verlag).

Hodell, D.A., 1993. Late Pleistocene paleoceanography of the South Atlantic sector of the Southern Ocean: Ocean Drilling Program Hole 704A. *Paleoceanography,* 8:47–67.

Howard, W.R., and Prell, W.L., 1992. Late Quaternary surface circulation of the southern Indian Ocean and its relationship to orbital variations. *Paleoceanography,* 7:79–117.

————————, 1994. Late Quaternary $CaCO_3$ production and preservation in the Southern Ocean: implications for oceanic and atmospheric carbon cycling, *Paleoceanography,* 9:453–482.

Imbrie, J., Hays, J.D., Martinson, D.G., McIntyre, A., Mix, A.C., Morley, J.J., Pisias, N.G., Prell, W.L., and Shackleton, N.J., 1984. The orbital theory of Pleistocene climate: support from a revised chronology of the marine $\delta^{18}O$ record. *In* Berger, A., Imbrie, J., Hays, J., Kukla, G., and Saltzman, B. (Eds.), *Milankovitch and Climate* (Pt. 1), NATO ASI Ser. C, Math Phys. Sci., 126:269–305.

Jansen, J.H.F., Kuijpers, A., and Troelstra, S.R., 1986. A mid-Brunhes climatic event: long-term changes in global atmospheric and ocean circulation. *Science,* 232:619–622.

Kipp, N.G., 1976. New transfer function for estimating past sea-surface conditions from sea-bed distribution of planktonic foraminiferal assemblages in the North Atlantic. *In* Cline, R.M., and Hays, J.D. (Eds.), *Investigation of Late Quaternary Paleoceanography and Paleoclimatology.* Mem.—Geol. Soc. Am., 145:3–41.

Little, M.G., Schneider, R.R., Kroon, D., Price, B., Bickert, T., and Wefer, G., 1997. Rapid paleoceanographic changes in the Benguela Upwelling System for the last 160,000 years as indicated by abundances of planktonic foraminifera. *Palaeogeogr., Palaeoclimatol., Palaeoecol.,* 130:135–161.

Lutjeharms, J.R.E., 1996. The exchange of water between the South Indian and South Atlantic Oceans. *In* Wefer, G., Berger, W.H., Siedler, G., and Webb, D.J. (Eds.), *The South Atlantic: Present and Past Circulation:* Berlin (Springer-Verlag), 125–162.

Lutjeharms, J.R.E., and Gordon, A.L., 1987. Shedding of an Agulhas ring observed at sea. *Nature,* 325:138–140.

Lutjeharms, J.R.E., and Meeuwis, J.M., 1987. The extent and variability of South-East Atlantic upwelling. *S. Afr. J. Mar. Sci.,* 5:51–62.

Lutjeharms, J.R.E., and Stockton, P.L., 1987. Kinematics of the upwelling front off southern Africa. *S. Afr. J. Mar. Sci.,* 5:35–49.

Niebler, H.-S., 1995. Reconstruction of paleo-environmental parameters using stable isotopes and faunal assemblages of planktonic foraminifera in the South Atlantic Ocean. *Ber. Polarforsch.,* 167.

Niebler, H.-S., and Gersonde, R., 1998. A planktic foraminiferal transfer function for the southern South Atlantic Ocean. *Mar. Micropaleontol.,* 34:213–234.

Parker, F.L., 1962. Planktonic foraminiferal species in Pacific sediments. *Micropaleontology,* 8:219–254.

Pether, J., 1994. Molluscan evidence for enhanced deglacial advection of Agulhas water in the Benguela current, off southwestern Africa. *Palaeogeogr., Palaeoclimatol., Palaeoecol.,* 111:99–117.

Rau, A.J., Lee-Thorp, J., Rogers, J., and Giraudeau, J., 1999. Late Quaternary fluctuations in the circulation patterns of the Southern Benguela System. *Internat. Union Quat. Res. XVB Int. Congr.,* 146.

Rogers, J., and Bremner, J.M., 1991. The Benguela ecosystem, Part VII: Marine geological aspects. *Mar. Biol. Annu. Rev.,* 29:1–85.

Shannon, L.V., 1985. The Benguela ecosystem, Part I: Evolution of the Benguela, physical features and processes. *Annu. Rev. Oceanogr. Mar. Biol.,* 23:105–182.

Shannon, L.V., Agenbag, J.J., Walker, N.D., and Lutjeharms, J.R.E., 1990. A major perturbation in the Agulhas retroflection area in 1986. *Deep-Sea Res.,* 37:493–512.

Shannon, L.V., and Nelson, G., 1996. The Benguela: large scale features and processes and system variability. *In* Wefer, G., Berger, W.H., Siedler, G., Webb, D.J. (Eds.), *The South Atlantic: Present and Past Circulation:* Berlin (Springer-Verlag), 163–210.

Shipboard Scientific Party, 1998. Site 1087. *In* Wefer, G., Berger, W.H., and Richter, C., et al., *Proc. ODP, Sci. Results,* 175: College Station, TX (Ocean Drilling Program), 457–484.

————————, 1999. Leg 177 summary: Southern Ocean paleoceanography. *In* Gersonde, R., Hodell, D.A., Blum, P., et al., *Proc. ODP, Init. Repts.,* 177: College Station, TX (Ocean Drilling Program), 1–67.

Ufkes, E., Jansen, J.H.F., and Brummer, G.-J.A., 1998. Living planktonic foraminifera in the eastern South Atlantic during spring: indicators of water masses, upwelling and the Congo (Zaire) River Plume. *Mar. Micropaleontol.,* 33:27–53.

Figure F1. Schematic circulation setting around southern Africa (adapted from Pether, 1994, after Shannon, 1985, and Lutjeharms and Stockton, 1987) and location of Site 1087 (star). SAA = South Atlantic Anticyclone, SIA = South Indian Anticyclone, STC = Subtropical Convergence, F = offshore limit of the filamentous mixing domain.

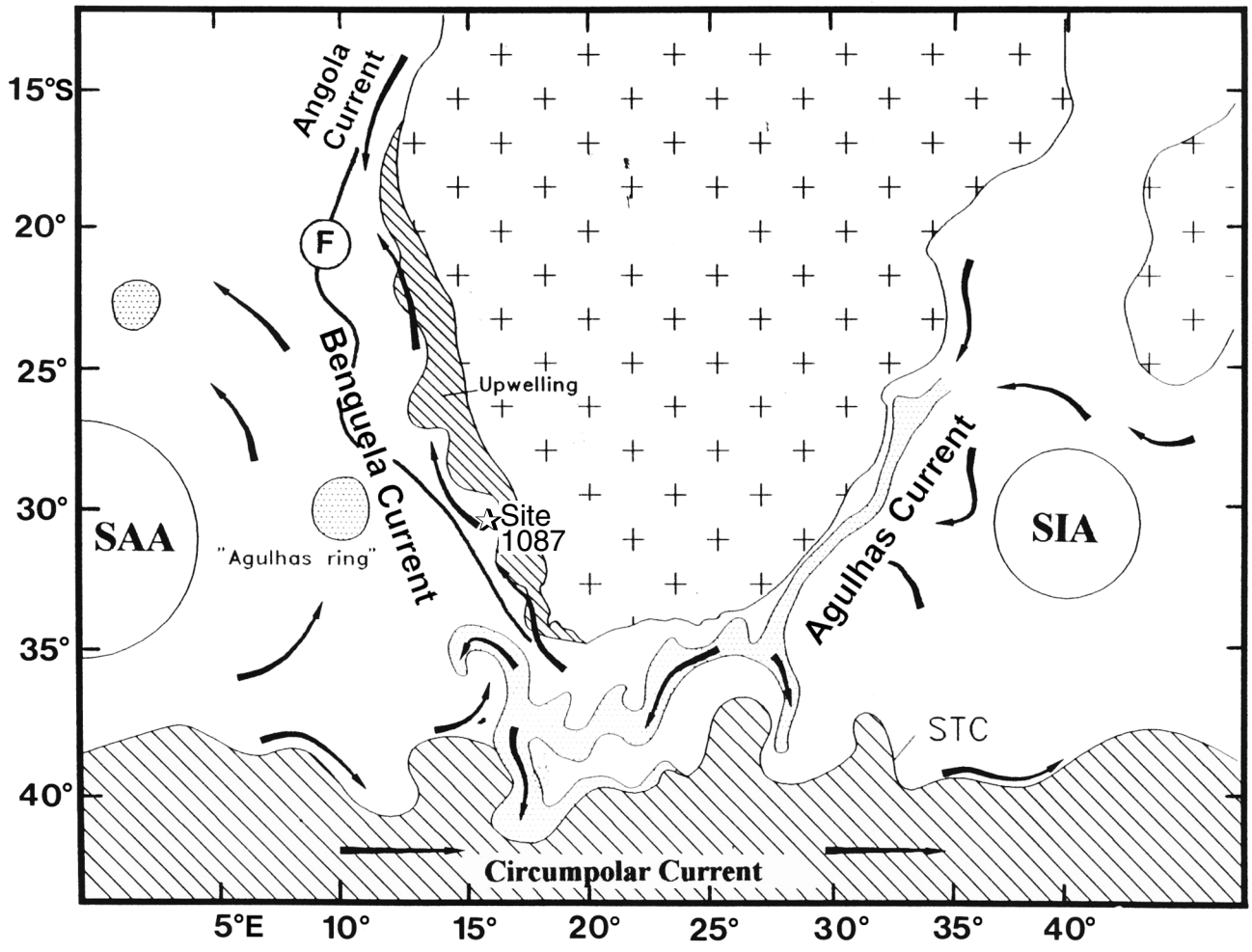

Figure F2. Oxygen isotope depth profile for Hole 1087A derived from measurements on the benthic foraminifer *C. wuellerstorfi*. Age control points (asterisks) are shown to the right of the $\delta^{18}O$ profile.

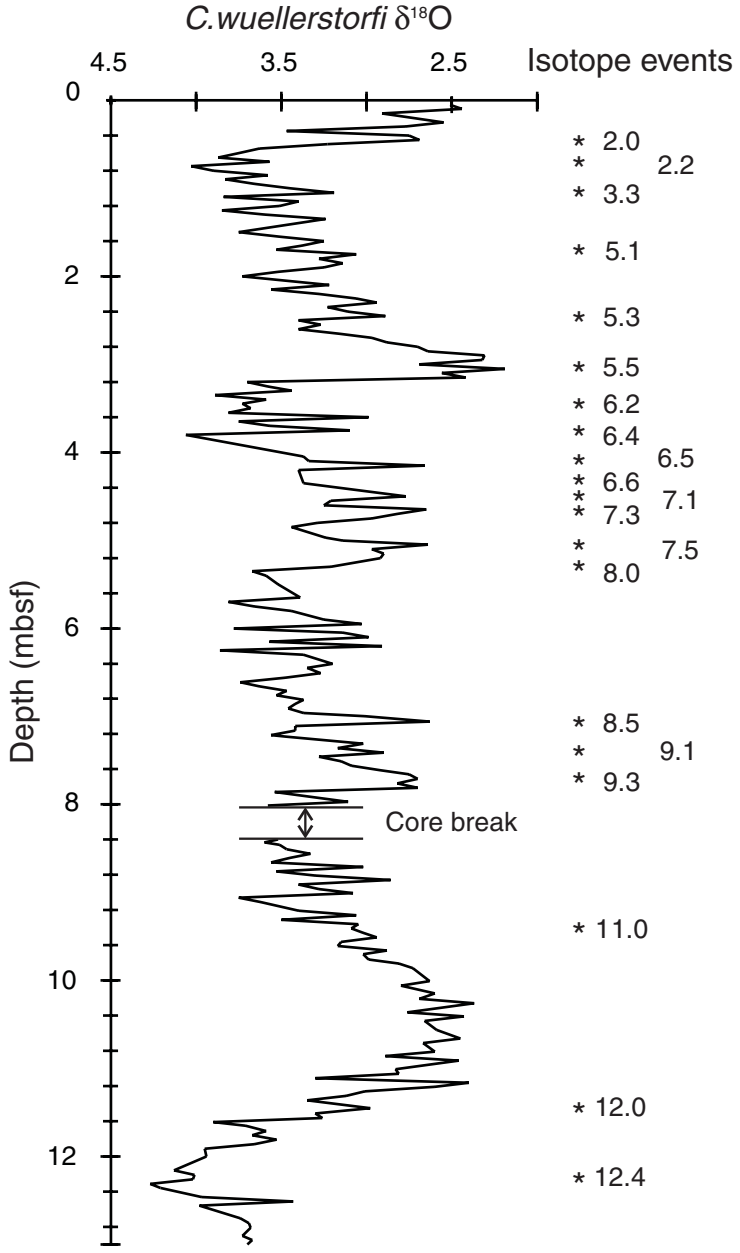

Figure F3. Relative abundances of the eight major species of planktonic foraminifers at Hole 1087A throughout the last 460 k.y. The original records have been smoothed (two points running average). Glacial isotope stages (shaded) are given on the right for reference.

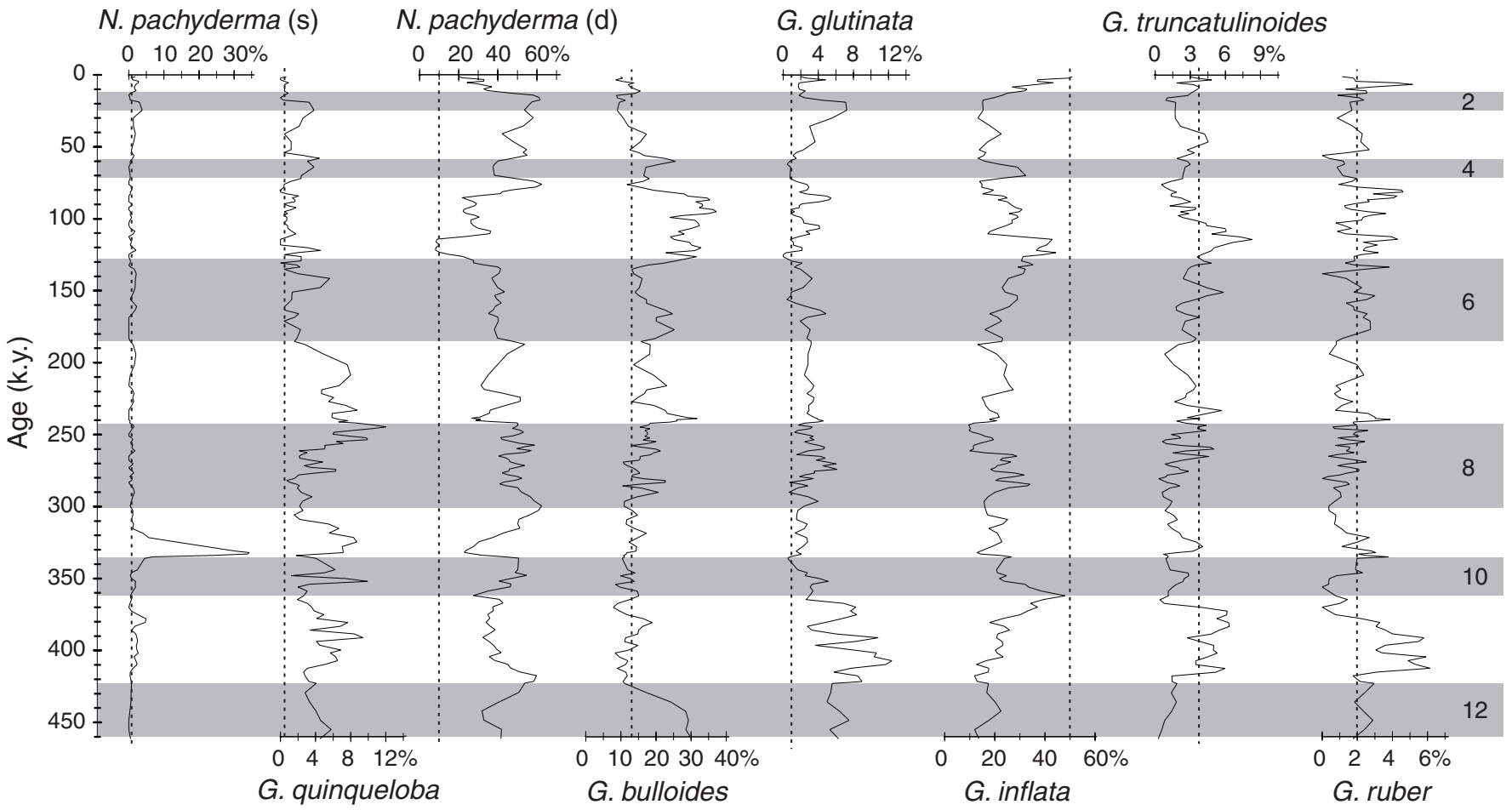

Figure F4. A. Concentrations and accumulation rates of *G. menardii* at Hole 1087A. Approximate ages of the *G. menardii* zonal boundary for the tropical Atlantic are from Ericson and Wollin (1968) and Briskin and Berggren (1975). **B.** Coiling ratio of *G. truncatulinoides* at Hole 1087A.

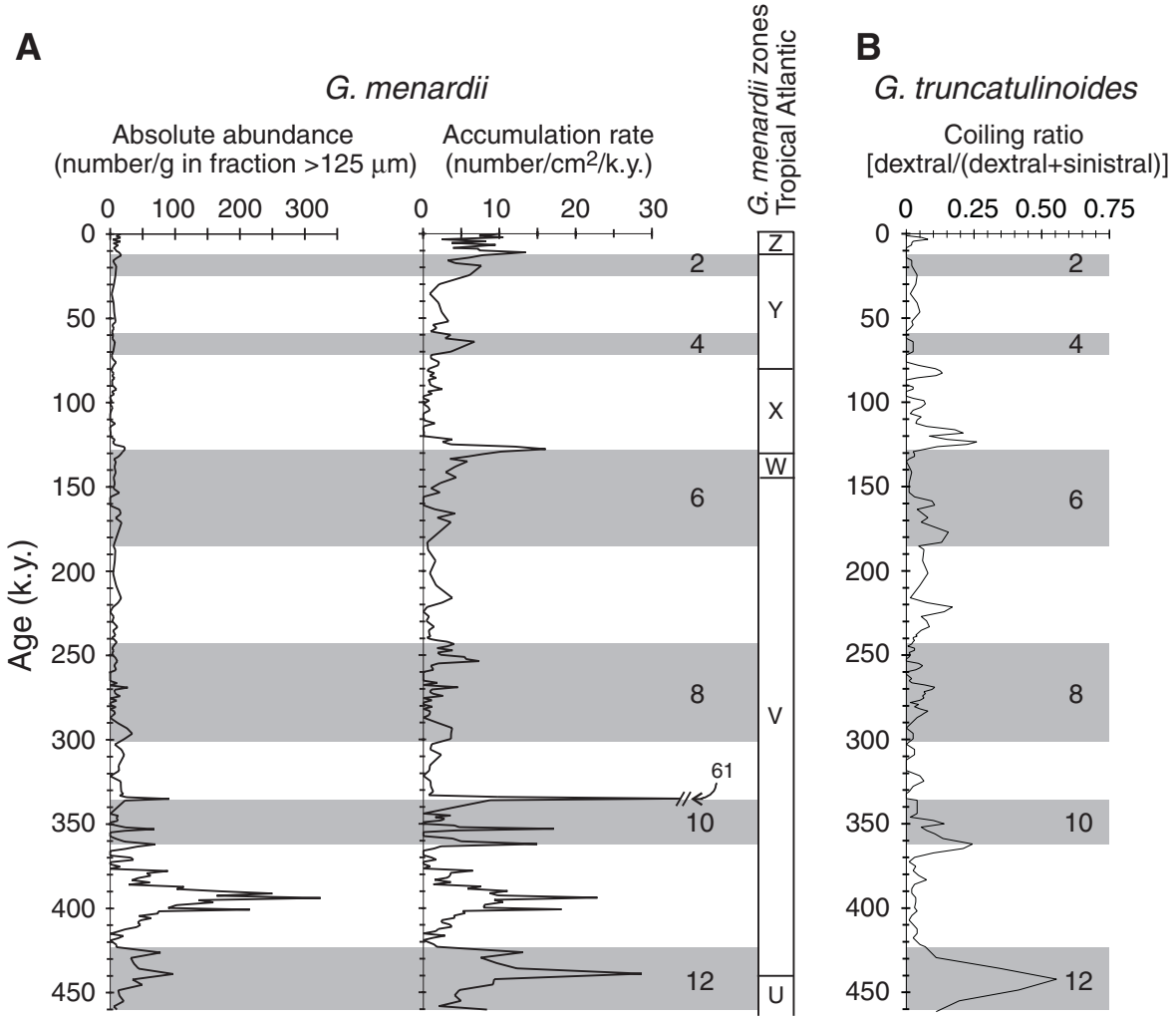

Table T1. Census counts of planktonic foraminifers at Hole 1087A. (Continued on next five pages.)

Core, section, interval (cm)	Depth (mbsf)	Total specimens counted	*N. pachyderma* (s)	*N. pachyderma* (d)	*G. bulloides*	*G. quinqueloba*	*G. scitula*	*G. glutinata*	*G. inflata*	*G. aequilateralis*	*G. falconensis*	*G. hirsuta*	*G. truncatulinoides*	*G. ruber*	*O. universa*	*G. sacculifer*	*N. dutertrei*	*G. calida*	*G. crassaformis*	Coiling (dextral/dextral+sinistral) *G. truncatulinoides*
175-1087A-																				
1H-1, 0-1	0	150	4	36	14	2	0	6	64	0	4	0	6	2	0	2	6	4	0	0
1H-1, 5-6	0.05	210	2	34	22	0	2	0	124	2	6	2	4	2	2	2	2	2	2	0
1H-1, 10-11	0.1	230	2	62	24	0	2	12	92	0	4	0	12	6	0	8	4	0	2	0.11
1H-1, 15-16	0.15	180	2	70	12	0	4	8	62	0	0	2	8	2	0	4	0	2	4	0.05
1H-1, 20-21	0.2	224	10	60	32	2	0	4	88	2	0	2	4	6	0	8	2	2	2	0
1H-1, 25-26	0.25	212	2	46	28	2	0	4	100	0	2	4	4	12	0	4	0	4	0	0.04
1H-1, 30-31	0.3	258	8	102	28	0	4	4	68	0	6	0	12	12	0	2	4	6	2	0
1H-1, 38-39	0.38	204	0	70	30	2	4	4	56	0	4	0	6	2	2	14	4	2	4	0
1H-1, 45-46	0.45	236	8	74	32	0	0	4	90	2	0	0	10	4	0	0	10	2	0	0
1H-1, 50-51	0.5	240	2	92	42	2	0	8	62	4	0	2	6	8	4	0	8	0	0	0
1H-1, 55-56	0.55	226	0	122	24	2	2	2	54	2	0	0	8	4	0	4	2	0	0	0
1H-1, 60-61	0.6	292	0	182	20	0	4	8	64	0	2	0	6	0	2	2	2	0	0	0
1H-1, 65-66	0.65	288	2	172	32	0	0	6	50	2	0	2	0	12	8	0	2	0	0	0.04
1H-1, 70-71	0.7	332	0	212	38	2	0	22	44	2	4	0	6	2	0	0	0	0	0	0
1H-1, 75-76	0.75	236	14	120	18	14	2	18	40	0	0	0	4	6	0	0	0	0	0	0.04
1H-1, 80-81	0.8	234	4	132	24	4	4	16	32	0	2	6	4	2	0	0	4	0	0	0.04
1H-1, 85-86	0.85	234	2	140	26	8	2	10	30	0	2	0	4	2	2	0	2	4	0	0.03
1H-1, 90-91	0.9	228	4	106	30	2	0	4	54	0	2	2	6	6	4	2	2	4	0	0
1H-1, 95-96	0.95	206	4	78	44	0	0	10	44	0	0	4	12	4	2	0	0	4	0	0.08
1H-1, 100-101	1	246	2	142	24	6	6	6	32	2	0	6	8	6	2	0	0	4	0	0.02
1H-1, 105-106	1.05	274	2	142	42	0	4	6	40	2	2	6	6	8	8	2	0	4	0	0.02
1H-1, 110-111	1.1	266	2	144	40	2	0	2	48	0	0	0	12	0	4	2	2	6	2	0.03
1H-1, 115-116	1.15	272	6	152	50	12	0	4	36	0	2	0	2	0	0	0	6	0	2	0
1H-1, 120-121	1.2	268	0	108	72	12	4	4	36	0	4	2	8	2	8	0	6	0	2	0
1H-1, 125-126	1.25	240	2	96	58	4	0	0	44	0	4	2	6	4	10	4	0	2	4	0
1H-1, 130-131	1.3	228	0	84	40	12	10	2	58	2	2	2	8	2	0	0	0	2	4	0
1H-1, 135-136	1.35	252	0	96	42	6	0	2	82	2	0	0	4	2	6	2	2	4	2	0.05
1H-2, 0-1	1.5	256	2	98	42	6	0	2	82	0	4	0	8	4	2	0	0	0	6	0
1H-2, 5-6	1.55	254	0	146	50	6	0	2	30	0	2	0	4	6	4	0	2	2	0	0
1H-2, 10-11	1.6	188	0	110	24	0	2	4	30	0	2	6	2	2	0	0	2	4	0	0
1H-2, 15-16	1.65	244	0	162	26	2	4	8	34	0	0	4	0	2	2	0	0	0	0	0
1H-2, 20-21	1.7	232	4	122	48	0	0	6	36	0	2	0	4	8	0	0	0	0	2	0.09

Table T1 (continued).

Core, section, interval (cm)	Depth (mbsf)	Total specimens counted	*N. pachyderma* (s)	*N. pachyderma* (d)	*G. bulloides*	*G. quinqueloba*	*G. scitula*	*G. glutinata*	*G. inflata*	*G. aequilateralis*	*G. falconensis*	*G. hirsuta*	*G. truncatulinoides*	*G. ruber*	*O. universa*	*G. sacculifer*	*N. dutertrei*	*G. calida*	*G. crassaformis*	Coiling (dextral/dextral+sinistral) *G. truncatulinoides*
1H-2, 25-26	1.75	214	0	90	38	0	2	6	50	0	2	2	2	12	0	0	4	0	6	0.13
1H-2, 30-31	1.8	222	2	94	66	0	2	2	28	0	0	2	6	8	0	2	4	2	4	0.13
1H-2, 35-36	1.85	272	0	110	72	4	0	12	48	2	2	2	0	6	0	2	2	2	8	0.14
1H-2, 40-41	1.9	222	0	44	70	6	0	12	64	0	0	0	6	14	2	0	2	2	0	0.08
1H-2, 45-46	1.95	218	0	52	82	0	2	12	46	4	4	0	4	4	2	0	0	0	6	0
1H-2, 50-51	2	242	0	60	80	8	8	12	52	0	0	0	8	8	2	0	0	2	2	0
1H-2, 55-56	2.05	290	0	86	86	0	2	10	82	0	4	2	8	6	0	0	2	0	2	0
1H-2, 60-61	2.1	252	4	72	92	2	2	2	60	0	0	0	4	4	0	0	0	6	4	0
1H-2, 65-66	2.15	212	0	60	64	2	4	6	64	0	0	0	2	2	0	0	6	2	0	0.05
1H-2, 70-71	2.2	232	0	54	80	6	2	2	62	0	2	0	14	4	0	0	2	0	4	0
1H-2, 75-76	2.25	252	0	56	96	0	0	2	88	2	0	0	2	4	0	0	0	0	2	0
1H-2, 80-81	2.3	226	2	50	82	2	0	4	56	0	6	0	8	8	0	0	2	0	6	0
1H-2, 85-86	2.35	270	0	68	90	2	0	0	72	2	0	0	6	10	2	6	10	0	2	0
1H-2, 90-91	2.4	234	2	72	50	0	0	6	72	0	2	0	4	4	6	2	2	6	6	0.05
1H-2, 95-96	2.45	272	2	82	72	4	4	4	76	2	2	0	8	8	0	2	4	0	2	0.08
1H-2, 100-101	2.5	258	0	58	92	0	0	8	66	2	4	2	10	4	2	2	2	0	6	0.06
1H-2, 105-106	2.55	254	0	76	72	2	0	4	72	0	2	2	12	0	0	4	4	2	2	0.05
1H-2, 110-111	2.6	242	0	60	88	2	4	16	50	0	0	0	10	6	4	0	0	0	2	0
1H-2, 115-116	2.65	230	2	80	54	2	6	4	50	0	2	6	18	2	2	0	0	2	0	0.03
1H-2, 120-121	2.7	232	6	88	68	4	4	8	34	0	0	2	10	2	2	0	0	0	4	0.08
1H-2, 125-126	2.75	224	0	76	60	4	2	6	44	0	0	2	12	4	8	0	2	2	2	0
1H-2, 130-131	2.8	262	0	36	56	0	2	2	106	0	0	4	24	16	2	0	6	2	6	0.07
1H-2, 135-136	2.85	242	2	10	70	0	6	2	110	2	2	6	18	6	0	2	0	0	6	0.08
1H-2, 140-141	2.9	272	2	34	82	0	2	4	104	0	2	2	16	6	2	2	6	2	6	0.28
1H-2, 145-146	2.95	246	0	20	74	0	2	2	106	0	0	2	14	10	4	0	4	0	8	0.14
1H-3, 0-1	3	230	6	20	82	14	2	8	74	2	0	0	10	2	0	2	2	2	4	0.03
1H-3, 5-6	3.05	264	4	20	70	8	2	2	108	0	0	10	14	10	2	4	6	2	2	0.27
1H-3, 10-11	3.1	230	0	30	44	2	6	0	110	2	2	0	8	6	8	4	6	0	2	0.25
1H-3, 15-16	3.15	230	0	40	82	0	0	0	70	2	2	0	10	4	8	2	6	4	0	0.2
1H-3, 20-21	3.2	212	0	56	58	10	4	0	68	0	0	0	6	4	2	0	4	0	0	0.03
1H-3, 30-31	3.3	220	2	64	52	0	2	4	64	0	2	0	12	4	10	0	2	2	0	0.02
1H-3, 35-36	3.35	240	0	62	50	0	2	6	92	0	0	0	10	2	4	2	8	2	0	0.04
1H-3, 40-41	3.4	218	0	84	32	8	2	2	70	2	0	0	6	6	2	2	2	0	0	0.02

Table T1 (continued).

Core, section, interval (cm)	Depth (mbsf)	Total specimens counted	*N. pachyderma* (s)	*N. pachyderma* (d)	*G. bulloides*	*G. quinqueloba*	*G. scitula*	*G. glutinata*	*G. inflata*	*G. aequilateralis*	*G. falconensis*	*G. hirsuta*	*G. truncatulinoides*	*G. ruber*	*O. universa*	*G. sacculifer*	*N. dutertrei*	*G. calida*	*G. crassaformis*	Coiling (dextral/dextral+sinistral) *G. truncatulinoides*
1H-3, 45-46	3.45	244	2	100	38	2	2	4	64	0	2	0	8	12	2	2	6	0	0	0
1H-3, 50-51	3.5	262	6	110	28	0	0	6	100	0	0	0	6	0	2	0	0	2	2	0
1H-3, 55-56	3.55	204	4	80	34	8	4	6	50	0	0	0	6	0	4	2	0	2	4	0.02
1H-3, 60-61	3.6	220	4	76	34	16	2	8	58	0	4	0	4	6	0	2	0	2	4	0.02
1H-3, 70-71	3.7	226	4	102	34	4	2	2	44	0	2	0	16	4	0	0	0	10	2	0
1H-3, 75-76	3.75	216	2	90	28	2	2	2	62	0	2	0	10	4	4	0	2	6	0	0.02
1H-3, 80-81	3.8	240	2	84	42	4	2	2	70	0	2	0	10	10	8	0	0	4	0	0
1H-3, 85-86	3.85	222	0	98	38	2	0	0	64	0	2	0	6	2	0	0	4	4	2	0.06
1H-3, 90-91	3.9	218	6	86	38	2	2	6	56	0	0	2	4	4	0	0	2	6	4	0.13
1H-3, 95-96	3.95	232	4	88	52	0	2	6	60	0	0	0	4	4	4	0	4	4	0	0.08
1H-3, 100-101	4	208	4	78	48	2	8	12	38	2	2	0	4	4	0	0	2	4	0	0
1H-3, 105-106	4.05	250	0	82	66	8	4	10	44	0	4	0	8	8	2	4	4	6	0	0.12
1H-3, 110-111	4.1	276	0	130	38	0	0	4	68	0	2	0	12	4	8	2	4	2	2	0.04
1H-3, 115-116	4.15	250	0	84	66	2	6	6	52	0	2	0	2	10	2	12	6	0	0	0.07
1H-3, 120-121	4.2	266	0	114	64	10	10	10	30	0	2	0	10	4	0	4	4	2	2	0.24
1H-3, 125-126	4.25	244	0	90	38	0	2	4	86	0	0	0	8	2	2	2	2	2	6	0.02
1H-3, 130-131	4.3	254	2	146	40	8	2	12	26	0	2	0	8	2	0	2	2	2	0	0.07
1H-3, 135-136	4.35	248	4	124	52	6	6	4	40	0	2	0	2	2	0	0	0	6	0	0.06
1H-4, 0-1	4.5	246	6	98	38	18	4	10	62	0	2	0	2	0	0	2	2	0	2	0.06
1H-4, 5-6	4.55	254	2	102	30	20	8	4	62	0	0	0	6	10	2	2	2	2	2	0.1
1H-4, 10-11	4.6	246	0	74	66	20	4	8	56	0	2	0	8	2	0	0	4	2	0	0
1H-4, 15-16	4.65	268	0	88	52	14	2	10	78	0	2	0	10	2	2	2	6	0	0	0.03
1H-4, 20-21	4.7	288	6	96	44	12	4	8	74	0	2	0	8	4	4	10	6	10	0	0.12
1H-4, 25-26	4.75	232	2	120	42	12	0	6	38	0	2	0	6	0	0	0	2	2	0	0.22
1H-4, 30-31	4.8	316	4	162	36	22	6	14	42	0	0	0	8	6	0	8	2	6	0	0.06
1H-4, 35-36	4.85	252	4	130	38	10	0	6	46	0	2	0	2	4	0	8	0	2	0	0.05
1H-4, 40-41	4.9	294	0	110	70	32	6	10	42	0	0	0	14	2	0	2	2	4	0	0.1
1H-4, 46-47	4.96	242	0	84	52	16	0	6	52	0	2	0	16	2	0	4	2	6	0	0.07
1H-4, 50-51	5	272	0	100	68	14	0	8	56	0	0	0	6	12	0	0	6	2	0	0.04
1H-4, 55-56	5.05	244	0	60	80	16	4	10	56	0	2	0	8	4	2	0	0	2	0	0.03
1H-4, 60-61	5.1	274	0	78	84	16	4	10	42	0	0	0	12	12	2	2	6	6	0	0.05
1H-4, 65-66	5.15	236	0	80	50	18	6	10	48	2	2	0	2	8	0	2	4	4	0	0
1H-4, 70-71	5.2	284	2	66	88	22	0	14	60	0	0	0	8	8	2	2	4	8	0	0.05

Table T1 (continued).

Core, section, interval (cm)	Depth (mbsf)	Total specimens counted	*N. pachyderma* (s)	*N. pachyderma* (d)	*G. bulloides*	*G. quinqueloba*	*G. scitula*	*G. glutinata*	*G. inflata*	*G. aequilateralis*	*G. falconensis*	*G. hirsuta*	*G. truncatulinoides*	*G. ruber*	*O. universa*	*G. sacculifer*	*N. dutertrei*	*G. calida*	*G. crassaformis*	Coiling (dextral/dextral+sinistral) *G. truncatulinoides*
1H-4, 75-76	5.25	256	0	132	44	14	2	8	36	2	0	0	4	2	2	6	2	2	0	0.01
1H-4, 80-81	5.3	368	2	178	72	44	4	6	34	0	0	0	14	10	0	0	4	0	0	0.04
1H-4, 85-86	5.35	324	6	170	52	30	0	6	32	0	0	0	16	4	2	0	2	4	0	0
1H-4, 90-91	5.4	338	4	156	50	50	10	16	34	0	4	0	8	0	4	0	0	2	0	0.01
1H-4, 95-96	5.45	286	2	140	62	18	2	4	30	0	0	0	14	4	2	4	0	4	0	0.05
1H-4, 100-101	5.5	316	2	170	38	32	6	6	28	0	0	0	12	12	2	4	2	2	0	0.01
1H-4, 105-106	5.55	294	0	154	68	6	6	2	40	2	0	0	6	0	4	2	0	4	0	0.01
1H-4, 110-111	5.6	282	0	140	34	28	10	12	42	0	2	0	2	10	0	0	0	2	0	0.02
1H-4, 115-116	5.65	306	0	140	66	18	4	8	52	0	0	0	10	2	0	0	4	2	0	0
1H-4, 120-121	5.7	350	6	130	52	48	4	12	72	0	2	2	4	4	4	4	0	6	0	0
1H-4, 125-126	5.75	326	2	154	58	20	2	12	60	0	0	0	2	6	8	0	0	2	0	0
1H-4, 130-131	5.8	332	2	154	74	22	8	4	50	0	2	0	2	10	2	2	0	0	0	0.09
1H-4, 135-136	5.85	288	2	160	36	22	6	14	36	0	2	0	4	2	0	2	0	2	0	0.03
1H-4, 140-141	5.9	248	4	154	34	6	2	8	26	0	0	0	8	2	0	0	2	2	0	0.07
1H-4, 145-146	5.95	258	0	116	46	20	2	16	32	0	0	0	16	6	2	2	0	0	0	0
1H-5, 0-1	6	262	6	142	58	6	2	8	28	0	0	0	10	2	0	0	0	0	0	0
1H-5, 5-6	6.05	304	4	182	62	6	0	8	28	0	0	0	4	6	0	0	2	0	2	0
1H-5, 10-11	6.1	242	2	114	44	10	2	4	54	0	0	0	4	4	0	0	2	2	0	0.02
1H-5, 15-16	6.15	288	0	114	54	2	4	4	92	0	0	0	14	0	0	0	0	4	0	0.02
1H-5, 20-21	6.2	280	0	116	34	10	2	20	72	0	0	0	12	2	2	2	0	6	2	0
1H-5, 25-26	6.25	244	0	114	46	2	8	6	50	2	0	0	6	4	0	6	0	0	0	0.04
1H-5, 30-31	6.3	276	0	124	32	16	6	14	66	0	0	0	6	6	2	0	0	4	0	0.1
1H-5, 35-36	6.35	208	2	98	20	8	2	10	60	0	0	0	2	6	0	0	0	0	0	0.11
1H-5, 40-41	6.4	276	4	142	34	10	0	20	54	0	0	4	2	0	0	0	0	6	0	0.08
1H-5, 45-46	6.45	344	0	192	40	6	2	6	76	0	0	0	6	6	2	0	2	6	0	0.05
1H-5, 50-51	6.5	270	0	120	40	14	2	24	50	0	0	0	6	4	4	0	0	6	0	0.09
1H-5, 55-56	6.55	296	2	140	40	22	6	10	54	0	2	0	6	8	2	0	0	4	0	0.03
1H-5, 60-61	6.6	272	4	120	44	14	2	10	58	2	0	0	10	4	0	0	0	2	2	0.1
1H-5, 65-66	6.65	288	4	116	42	8	0	10	100	0	0	0	2	4	0	0	0	2	0	0
1H-5, 70-71	6.7	314	0	156	38	4	0	4	90	0	0	2	4	2	4	2	6	2	0	0.03
1H-5, 75-76	6.75	326	2	162	46	8	0	8	88	0	2	0	2	0	2	0	2	4	0	0.06
1H-5, 80-81	6.8	270	4	148	50	2	2	12	46	0	0	0	0	0	0	0	2	4	0	0
1H-5, 85-86	6.85	298	0	130	80	2	0	0	70	0	0	0	4	4	0	0	2	6	0	0.1

Table T1 (continued).

Core, section, interval (cm)	Depth (mbsf)	Total specimens counted	*N. pachyderma* (s)	*N. pachyderma* (d)	*G. bulloides*	*G. quinqueloba*	*G. scitula*	*G. glutinata*	*G. inflata*	*G. aequilateralis*	*G. falconensis*	*G. hirsuta*	*G. truncatulinoides*	*G. ruber*	*O. universa*	*G. sacculifer*	*N. dutertrei*	*G. calida*	*G. crassaformis*	Coiling (dextral/dextral+sinistral) *G. truncatulinoides*
1H-5, 90-91	6.9	282	0	120	52	4	2	4	92	0	0	0	2	4	0	0	0	2	0	0.06
1H-5, 95-96	6.95	356	2	140	40	8	4	10	126	0	2	0	10	6	4	2	0	2	0	0.07
1H-5, 100-101	7	288	2	140	28	6	4	8	88	0	0	0	4	2	0	0	0	6	0	0.04
1H-5, 105-106	7.05	342	6	176	74	6	0	2	70	0	0	0	4	2	0	0	0	2	0	0.04
1H-5, 110-111	7.1	274	4	144	54	8	0	2	54	0	2	0	0	4	0	2	0	0	0	0
1H-5, 115-116	7.15	282	2	170	26	12	6	14	42	0	0	0	4	2	0	2	0	2	0	0
1H-5, 120-121	7.2	266	2	152	34	2	6	8	44	2	0	0	4	2	2	2	2	4	0	0.05
1H-5, 125-126	7.25	222	0	150	20	8	2	4	34	0	0	0	2	0	0	0	2	0	0	0
1H-5, 130-131	7.3	262	6	142	46	4	4	4	46	0	0	0	2	2	2	0	4	0	0	0
1H-5, 135-136	7.35	252	0	148	30	4	2	4	42	2	0	0	6	2	2	0	4	6	0	0.06
1H-5, 140-141	7.4	280	4	120	32	8	2	4	94	0	0	4	4	2	2	2	2	0	0	0
1H-5, 145-146	7.45	296	4	170	34	24	2	12	38	0	0	2	2	2	0	0	4	2	0	0
1H-6, 0-1	7.5	270	2	122	44	14	6	2	60	0	0	0	6	4	0	4	4	2	0	0
1H-6, 5-6	7.55	306	22	126	56	18	2	6	60	0	0	0	6	4	4	0	0	2	0	0
1H-6, 10-11	7.6	296	12	102	34	32	6	10	72	0	0	2	8	12	2	0	2	2	0	0.1
1H-6, 15-16	7.65	274	64	72	36	18	0	6	58	0	0	0	12	0	0	2	4	2	0	0.03
1H-6, 20-21	7.7	266	56	78	42	20	2	6	44	0	0	0	10	6	0	0	0	2	0	0.02
1H-6, 25-26	7.75	296	118	52	38	20	0	2	36	2	0	0	8	10	0	4	4	2	0	0
1H-6, 30-31	7.8	292	84	82	30	22	6	8	40	0	0	0	2	8	0	2	6	2	0	0
1H-6, 35-36	7.85	282	110	74	36	4	0	4	42	0	0	0	2	4	2	0	4	0	0	0
1H-6, 40-41	7.9	278	24	106	24	6	0	4	84	0	0	0	4	10	6	0	8	2	0	0
1H-6, 45-46	7.95	252	12	120	34	10	0	0	58	2	0	2	2	10	0	0	0	0	2	0
1H-6, 50-51	8	194	8	104	14	8	2	2	48	2	0	0	2	0	0	0	4	0	0	0.08
2H-1, 20-21	8.4	264	2	124	44	22	0	6	44	0	0	0	4	10	6	0	0	2	0	0
2H-1, 30-31	8.5	244	2	124	28	4	0	8	62	2	0	0	10	2	0	0	0	0	2	0.03
2H-1, 40-41	8.6	242	0	142	20	2	0	4	58	0	0	0	4	2	0	2	0	4	4	0.17
2H-1, 50-51	8.7	244	4	88	42	34	0	16	48	0	0	0	8	0	0	0	0	4	0	0.11
2H-1, 60-61	8.8	270	6	122	28	16	4	10	76	0	0	0	4	2	0	0	0	0	2	0
2H-1, 70-71	8.9	278	4	134	18	2	2	8	100	0	0	0	6	0	0	0	0	4	0	0.15
2H-1, 80-81	9	246	6	110	32	8	2	8	76	0	0	0	2	0	0	0	2	0	0	0.06
2H-1, 90-91	9.1	282	0	74	46	8	0	10	130	0	0	0	4	2	2	2	2	2	0	0.21
2H-1, 100-101	9.2	244	2	70	34	6	0	6	122	0	0	0	2	2	0	0	0	0	0	0.28
2H-1, 110-111	9.3	292	2	154	32	4	0	8	84	2	0	0	0	6	0	0	0	0	0	0.14

Table T1 (continued).

Core, section, interval (cm)	Depth (mbsf)	Total specimens counted	*N. pachyderma* (s)	*N. pachyderma* (d)	*G. bulloides*	*G. quinqueloba*	*G. scitula*	*G. glutinata*	*G. inflata*	*G. aequilateralis*	*G. falconensis*	*G. hirsuta*	*G. truncatulinoides*	*G. ruber*	*O. universa*	*G. sacculifer*	*N. dutertrei*	*G. calida*	*G. crassaformis*	Coiling (dextral/dextral+sinistral) *G. truncatulinoides*
2H-1, 120-121	9.4	252	0	82	18	12	2	28	100	0	0	0	4	0	0	2	0	2	2	0.06
2H-1, 130-131	9.5	256	0	108	22	6	0	14	88	2	0	0	16	0	0	0	0	0	0	0
2H-1, 140-141	9.6	264	4	88	28	14	0	26	84	0	0	0	16	2	0	0	0	2	0	0.02
2H-2, 0-1	9.7	260	10	94	34	12	0	18	74	0	0	0	16	2	0	0	0	0	0	0.05
2H-2, 10-11	9.8	274	16	98	54	10	0	18	50	0	0	0	12	10	0	2	2	2	0	0
2H-2, 20-21	9.9	342	12	110	62	40	0	10	60	0	0	0	28	10	0	2	2	2	4	0.09
2H-2, 30-31	10	312	0	124	44	6	2	8	94	0	0	0	14	10	2	2	4	2	0	0.06
2H-2, 40-41	10.1	250	4	94	40	12	0	10	54	0	0	0	16	10	2	2	4	2	0	0
2H-2, 50-51	10.2	250	6	84	34	30	2	20	52	0	0	0	8	10	0	0	2	2	0	0.04
2H-2, 60-61	10.3	264	6	82	24	18	2	36	54	0	0	0	6	20	4	4	6	2	0	0
2H-2, 70-71	10.4	292	8	116	38	4	2	8	74	0	0	0	16	10	4	6	4	2	0	0.07
2H-2, 80-81	10.5	264	4	94	44	20	0	12	56	0	0	0	12	10	2	4	2	2	2	0
2H-2, 92-93	10.62	260	8	114	20	16	0	30	50	0	0	0	14	6	0	0	0	2	0	0.06
2H-2, 100-101	10.7	268	6	106	24	14	0	26	60	2	0	0	14	12	0	2	2	0	0	0.02
2H-2, 110-111	10.8	272	2	86	28	20	2	30	66	0	0	0	10	20	0	2	0	4	2	0.02
2H-2, 120-121	10.9	248	8	112	34	14	2	34	22	0	0	0	8	6	0	0	4	4	0	0
2H-2, 130-131	11	268	4	120	24	12	0	26	44	0	0	0	10	22	2	0	4	0	0	0.05
2H-2, 140-141	11.1	244	2	118	22	4	2	14	46	0	0	0	20	10	2	2	0	2	0	0.03
2H-3, 0-1	11.2	276	0	148	38	10	4	16	44	0	0	0	6	6	0	0	0	4	0	0.05
2H-3, 10-11	11.3	304	2	200	30	6	0	34	24	0	0	0	2	4	0	0	0	2	0	0
2H-3, 25-26	11.45	266	2	136	30	12	0	18	48	0	0	0	6	8	2	2	2	0	0	0.1
2H-3, 30-31	11.5	274	2	154	30	10	0	12	46	0	0	0	4	8	0	2	2	4	0	0.04
2H-3, 40-41	11.6	310	2	140	74	6	0	20	52	0	0	0	4	6	2	2	0	2	0	0.18
2H-3, 50-51	11.7	342	2	126	84	16	0	12	80	4	0	0	8	6	0	0	2	2	0	0.51
2H-3, 60-61	11.8	408	0	110	132	14	2	38	88	0	0	0	2	12	2	0	0	8	0	0.6
2H-3, 70-71	11.9	352	0	136	92	20	2	20	48	2	0	0	4	10	4	2	0	12	0	0.23
2H-3, 80-81	12	408	0	184	126	24	0	20	42	0	0	0	0	8	0	0	0	4	0	0.16
2H-3, 90-91	12.1	388	4	148	114	12	2	30	66	0	0	0	2	6	2	0	0	2	0	0.06

Table T2. Concentrations and accumulation rates of *Globorotalia menardii* at Hole 1087A (Continued on next page.).

Core, section, interval (cm)	Depth (mbsf)	Number/ g bulk sediment	Number/cm²/k.y.
175-1087A-			
1H-1, 0-1	0.00	2.40	10.13
1H-1, 5-6	0.05	1.73	7.33
1H-1, 10-11	0.10	2.48	10.50
1H-1, 15-16	0.15	0.57	2.39
1H-1, 20-21	0.20	1.95	8.23
1H-1, 25-26	0.25	0.88	3.71
1H-1, 30-31	0.30	2.24	9.48
1H-1, 38-39	0.38	0.92	3.89
1H-1, 40-41	0.40	1.72	7.27
1H-1, 45-46	0.45	1.73	7.30
1H-1, 50-51	0.50	3.18	13.43
1H-1, 55-56	0.55	3.55	7.79
1H-1, 60-61	0.60	2.74	6.01
1H-1, 65-66	0.65	1.46	3.20
1H-1, 70-71	0.70	1.92	4.20
1H-1, 75-76	0.75	3.46	7.60
1H-1, 80-81	0.80	2.77	6.08
1H-1, 85-86	0.85	1.86	2.07
1H-1, 90-91	0.90	0.77	0.85
1H-1, 95-96	0.95	1.80	2.00
1H-1, 100-101	1.00	2.16	2.40
1H-1, 105-106	1.05	2.98	3.31
1H-1, 110-111	1.10	1.15	1.28
1H-1, 115-116	1.15	1.58	1.75
1H-1, 120-121	1.20	0.86	0.95
1H-1, 125-126	1.25	1.17	3.59
1H-1, 130-131	1.30	0.93	2.88
1H-1, 135-136	1.35	2.19	6.73
1H-2, 0-1	1.50	1.17	3.60
1H-2, 5-6	1.55	0.33	1.01
1H-2, 10-11	1.60	0.32	0.99
1H-2, 15-16	1.65	0.77	2.06
1H-2, 20-21	1.70	0.72	1.92
1H-2, 25-26	1.75	0.28	0.75
1H-2, 30-31	1.80	0.20	0.53
1H-2, 35-36	1.85	0.55	1.46
1H-2, 40-41	1.90	0.32	0.84
1H-2, 45-46	1.95	0.63	1.68
1H-2, 50-51	2.00	0.25	0.65
1H-2, 55-56	2.05	0.33	0.88
1H-2, 60-61	2.10	0.33	0.87
1H-2, 65-66	2.15	0.58	1.55
1H-2, 70-71	2.20	0.94	2.50
1H-2, 75-76	2.25	0.24	0.63
1H-2, 80-81	2.30	0.43	1.14
1H-2, 85-86	2.35	0.00	0.00
1H-2, 90-91	2.40	0.00	0.00
1H-2, 95-96	2.45	0.29	0.76
1H-2, 100-101	2.50	0.00	0.00
1H-2, 105-106	2.55	0.26	0.68
1H-2, 110-111	2.60	0.32	0.86
1H-2, 115-116	2.65	0.00	0.00
1H-2, 120-121	2.70	0.00	0.00
1H-2, 125-126	2.75	0.00	0.00
1H-2, 130-131	2.80	0.57	1.52
1H-2, 135-136	2.85	0.00	0.00
1H-2, 140-141	2.90	0.00	0.00
1H-2, 145-146	2.95	0.04	0.12
1H-3, 0-1	3.00	0.00	0.00
1H-3, 5-6	3.05	1.42	3.78
1H-3, 10-11	3.10	0.94	2.50
1H-3, 15-16	3.15	1.36	3.62
1H-3, 20-21	3.20	5.56	12.06
1H-3, 25-26	3.25	7.39	16.05
1H-3, 30-31	3.30	4.69	10.17
1H-3, 35-36	3.35	3.59	7.79
1H-3, 40-41	3.40	2.74	5.95
1H-3, 45-46	3.45	1.62	3.51
1H-3, 50-51	3.50	2.67	5.79
1H-3, 55-56	3.55	1.94	4.21
1H-3, 60-61	3.60	1.35	2.94
1H-3, 65-66	3.65	1.99	4.31
1H-3, 70-71	3.70	1.03	2.24
1H-3, 75-76	3.75	0.47	1.02
1H-3, 80-81	3.80	0.99	2.16
1H-3, 85-86	3.85	0.00	0.00
1H-3, 90-91	3.90	0.00	0.00
1H-3, 95-96	3.95	0.00	0.00
1H-3, 100-101	4.00	0.71	1.53
1H-3, 105-106	4.05	1.91	4.14
1H-3, 110-111	4.10	0.85	1.84
1H-3, 115-116	4.15	1.66	3.60
1H-3, 125-126	4.25	0.23	0.50
1H-3, 130-131	4.30	0.27	0.58
1H-3, 135-136	4.35	0.27	0.59
1H-4, 0-1	4.50	0.99	1.59
1H-4, 5-6	4.55	0.54	0.86
1H-4, 10-11	4.60	1.05	1.68
1H-4, 15-16	4.65	2.37	3.81
1H-4, 20-21	4.70	1.55	2.48
1H-4, 25-26	4.74	0.31	0.50
1H-4, 30-31	4.80	0.00	0.00
1H-4, 35-36	4.85	0.47	0.75
1H-4, 40-41	4.90	0.25	0.40
1H-4, 46-47	4.95	0.88	1.41
1H-4, 50-51	5.00	0.44	0.71
1H-4, 55-56	5.05	0.51	0.82
1H-4, 60-61	5.10	0.60	0.96
1H-4, 65-66	5.15	0.31	0.50
1H-4, 70-71	5.20	0.54	0.87
1H-4, 75-76	5.25	1.11	1.78
1H-4, 80-81	5.30	1.97	3.17
1H-4, 85-86	5.35	1.16	4.02
1H-4, 90-91	5.40	0.92	3.20
1H-4, 95-96	5.45	0.53	1.82
1H-4, 100-101	5.50	1.11	3.84
1H-4, 105-106	5.55	0.55	1.90
1H-4, 110-111	5.60	0.65	2.25
1H-4, 115-116	5.65	1.58	5.48
1H-4, 120-121	5.70	1.60	5.55
1H-4, 125-126	5.75	2.12	7.35
1H-4, 130-131	5.80	0.57	1.97
1H-4, 135-136	5.85	0.29	1.00
1H-4, 140-141	5.90	0.34	1.17
1H-4, 145-146	5.95	0.39	1.34
1H-5, 0-1	6.00	0.00	0.00
1H-5, 5-6	6.05	0.00	0.00
1H-5, 10-11	6.10	0.00	0.00
1H-5, 15-16	6.15	0.00	0.00
1H-5, 20-21	6.20	0.00	0.00
1H-5, 25-26	6.25	0.53	1.84
1H-5, 30-31	6.30	0.00	0.00
1H-5, 35-36	6.35	1.31	4.54
1H-5, 40-41	6.40	0.31	1.09
1H-5, 45-46	6.45	0.24	0.84
1H-5, 50-51	6.50	0.35	1.21
1H-5, 55-56	6.55	0.74	2.57
1H-5, 60-61	6.60	0.00	0.00
1H-5, 65-66	6.65	0.32	1.12
1H-5, 70-71	6.70	0.00	0.00
1H-5, 75-76	6.75	0.00	0.00
1H-5, 80-81	6.80	0.33	1.16
1H-5, 85-86	6.85	0.00	0.00
1H-5, 90-91	6.90	0.25	0.87
1H-5, 95-96	6.95	0.25	0.87

Table T2 (continued).

Core, section, interval (cm)	Depth (mbsf)	Number/ g bulk sediment	Number/cm²/k.y.
1H-5, 100-101	7.00	0.21	0.73
1H-5, 105-106	7.05	0.00	0.00
1H-5, 110-111	7.10	0.54	1.86
1H-5, 115-116	7.15	1.09	3.79
1H-5, 120-121	7.20	1.05	3.63
1H-5, 125-126	7.25	1.05	3.63
1H-5, 130-131	7.30	0.32	1.10
1H-5, 135-136	7.35	0.63	0.91
1H-5, 140-141	7.40	1.62	2.35
1H-6, 0-1	7.50	0.61	0.88
1H-6, 5-6	7.55	0.54	0.77
1H-6, 10-11	7.60	0.00	0.00
1H-6, 15-16	7.65	0.65	0.94
1H-6, 20-21	7.70	0.68	0.99
1H-6, 25-26	7.75	0.90	1.30
1H-6, 30-31	7.80	0.64	0.92
1H-6, 35-36	7.85	0.50	0.72
1H-6, 40-41	7.90	0.83	9.70
1H-6, 45-46	7.95	5.23	61.35
1H-6, 50-51	8.00	0.74	8.73
2H-1, 20-21	8.40	0.00	0.00
2H-1, 25-26	8.45	0.31	3.58
2H-1, 30-31	8.50	0.13	1.56
2H-1, 35-36	8.55	0.24	2.79
2H-1, 40-41	8.60	0.20	2.34
2H-1, 45-46	8.65	0.00	0.00
2H-1, 50-51	8.70	0.00	0.00
2H-1, 55-56	8.75	0.35	4.09
2H-1, 60-61	8.80	0.40	4.67
2H-1, 65-66	8.85	1.46	17.12
2H-1, 70-71	8.90	0.36	4.22
2H-1, 75-76	8.95	0.00	0.00
2H-1, 80-81	9.00	0.00	0.00
2H-1, 85-86	9.05	0.00	0.00
2H-1, 90-91	9.10	0.33	3.87
2H-1, 95-96	9.15	0.42	4.93
2H-1, 100-101	9.20	1.27	14.94
2H-1, 105-106	9.25	0.62	2.31
2H-1, 110-111	9.30	0.38	1.41
2H-1, 115-116	9.35	0.00	0.00
2H-1, 120-121	9.40	0.00	0.00
2H-1, 125-126	9.45	0.00	0.00
2H-1, 130-131	9.50	0.27	1.02
2H-1, 135-136	9.55	0.45	1.69
2H-1, 140-141	9.60	0.00	0.00
2H-1, 145-146	9.65	0.00	0.00
2H-2, 0-1	9.70	0.24	0.89
2H-2, 5-6	9.75	0.00	0.00
2H-2, 10-11	9.80	1.75	6.50
2H-2, 15-16	9.85	0.96	3.56
2H-2, 20-21	9.90	0.95	3.54
2H-2, 25-26	9.95	0.86	3.19
2H-2, 30-31	10.00	0.40	1.48
2H-2, 35-36	10.05	0.97	3.60
2H-2, 40-41	10.10	0.35	1.31
2H-2, 45-46	10.15	2.04	7.58
2H-2, 50-51	10.20	1.57	5.81
2H-2, 55-56	10.25	2.98	11.06
2H-2, 60-61	10.30	2.35	8.72
2H-2, 65-66	10.35	2.63	9.78
2H-2, 70-71	10.40	6.15	22.84
2H-2, 75-76	10.45	2.51	9.30
2H-2, 80-81	10.50	2.83	10.49
2H-2, 85-86	10.55	2.16	8.01
2H-2, 92-93	10.62	2.13	7.93
2H-2, 95-96	10.65	4.89	18.14
2H-2, 100-101	10.70	1.40	5.19
2H-2, 105-106	10.75	1.48	5.49
2H-2, 110-111	10.80	1.08	4.02
2H-2, 115-116	10.85	1.11	4.11
2H-2, 120-121	10.90	0.65	2.42
2H-2, 125-126	10.95	0.64	2.39
2H-2, 130-131	11.00	0.94	3.50
2H-2, 135-136	11.05	1.01	3.73
2H-2, 140-141	11.10	0.53	1.97
2H-2, 145-146	11.15	0.44	1.64
2H-3, 0-1	11.20	0.00	0.00
2H-3, 5-6	11.25	0.77	2.87
2H-3, 10-11	11.30	0.33	1.24
2H-3, 15-16	11.35	0.00	0.00
2H-3, 25-26	11.45	0.39	1.44
2H-3, 30-31	11.50	0.47	1.75
2H-3, 35-36	11.55	4.04	13.10
2H-3, 40-41	11.60	2.33	7.53
2H-3, 45-46	11.65	2.97	9.63
2H-3, 50-51	11.70	3.78	12.26
2H-3, 55-56	11.75	8.85	28.67
2H-3, 60-61	11.80	2.87	9.30
2H-3, 65-66	11.85	2.82	9.13
2H-3, 70-71	11.90	1.46	4.73
2H-3, 75-76	11.95	1.27	4.12
2H-3, 80-81	12.00	1.52	4.93
2H-3, 85-86	12.05	0.64	2.06
2H-3, 90-91	12.10	3.69	11.96
2H-3, 95-96	12.15	3.23	10.48
2H-3, 100-101	12.20	2.10	6.80
2H-3, 105-106	12.25	2.96	9.60
2H-3, 110-111	12.30	0.87	2.81
2H-3, 115-116	12.35	1.80	5.84

Table T3. Age control points for the benthic foraminiferal oxygen isotope record of Hole 1087A.

Isotope event	Depth (mbsf)	Age (ka)
2.0	50	11
2.2	75	19
3.3	105	52
5.1	175	80
5.3	245	99
5.5	305	122
6.2	350	135
6.4	375	151
6.5	415	171
6.6	425	183
7.1	450	194
7.3	465	216
7.5	505	238
8.0	530	242
8.5	705	287
9.1	740	309
9.3	775	331
11.0	920	362
12.0	1150	423
12.4	1225	471

Table T4. List of planktonic foraminiferal taxa and summary statistics of their relative percent abundance in the studied interval, Hole 1087A.

Species	Summary statistics (%)		
	Minimum	Maximum	Average
Neogloboquadrina pachyderma (d)	0	39.9	1.8
Neogloboquadrina pachyderma (s)	4.1	67.6	40.4
Globigerina bulloides	6.5	38.1	18
Globigerina quinqueloba	0	14.8	3.4
Globorotalia scitula	0	4.4	0.9
Globigerinita glutinata	0	13.7	3.3
Globorotalia inflata	7.9	59.1	23.2
Globigerinella aequilateralis	0	1.8	0.2
Globigerina falconensis	0	2.9	0.4
Globorotalia hirsuta	0	3.8	0.3
Globorotalia truncatulinoides	0	9.2	2.8
Globigerinoides ruber	0	8.2	2
Orbulina universa	0	4.6	0.6
Globigerinoides sacculifer	0	6.9	0.6
Neogloboquadrina dutertrei	0	4.2	0.8
Globigerinella calida	0	4.4	0.9
Globorotalia crassaformis	0	3.3	0.4